

1N-34  
107358

# The Effects of Acoustic Treatment on Pressure Disturbances From a Supersonic Jet in a Circular Duct

Milo D. Dahl  
*Lewis Research Center  
Cleveland, Ohio*

Prepared for the  
International Mechanical Engineering Congress and Exposition  
sponsored by the American Society of Mechanical Engineers  
Atlanta, Georgia, November 17-22, 1996



National Aeronautics and  
Space Administration



**THE EFFECTS OF ACOUSTIC TREATMENT ON  
PRESSURE DISTURBANCES FROM A SUPERSONIC JET  
IN A CIRCULAR DUCT**

**Milo D. Dahl**

NASA Lewis Research Center

Cleveland, OH 44135

**ABSTRACT**

The pressure disturbances generated by an instability wave in the shear layer of a supersonic jet are studied for an axisymmetric jet inside a lined circular duct. For the supersonic jet, locally linear stability analysis with duct wall boundary conditions is used to calculate the eigenvalues and the eigenfunctions at each axial location. These values are used to determine the growth rates and phase velocities of the instability waves and the near field pressure disturbance patterns. The study is confined to the dominant Kelvin-Helmholtz instability mode and to the region just downstream of the nozzle exit where the shear layer is growing but is still small in size compared to the radius of the duct. Numerical results are used to study the effects of changes in the outer flow, growth in the shear layer thickness, wall distance, and wall impedance, and the effects of these changes on non-axisymmetric modes. The primary results indicate that the effects of the duct wall on stability characteristics diminish as the outer flow increases and as the jet azimuthal mode number increases. Also, wall reflections are reduced when using a finite impedance boundary condition at the wall; but in addition, reflections are reduced and growth rates diminished by keeping the imaginary part of the impedance negative when using the negative exponential for the harmonic dependence.

## 1 INTRODUCTION

The effects of confining walls on supersonic jet mixing layers are important for combustion processes (Shin and Ferziger [1993]), for engine tests conducted inside an enclosed facility (Ahuja et al. [1992]), and for jet noise reduction efforts (Hu [1995]). In a circular configuration, the supersonic jet issues from a nozzle that has its axis coincident with the centerline of a surrounding circular duct. Between the jet and the confining wall of the duct, a lower speed outer flow exists. The shear layer between the two flows is initially thin and unstable. This instability grows like a wave as the flow moves downstream. As a result, this instability wave causes perturbations to spread into each flow away from the shear layer. Those perturbations that spread toward the wall can reflect off it and return toward the shear layer to interact and modify the growing instability in the shear layer. Thus the presence of the wall affects the characteristics of the instability waves that govern both the mixing in the high speed shear layer and the noise generation.

Compared to the many past experimental studies of ejectors and shrouded jets, the analysis of confined shear layers using stability theory has only begun recently. Tam and Hu [1989] studied the supersonic mixing layer inside a rectangular channel with hard walls. In addition to the Kelvin-Helmholtz (KH) instabilities, they found from using a vortex sheet model that the coupling of the unsteady motion with acoustic modes reflected from the walls resulted in a new family of supersonic instabilities with supersonic convective Mach number. The analysis also included the effects of shear layer thickness on the spatial growth rates of two- and three-dimensional supersonic instability waves. Zhuang et al. [1990] showed for a constant shear layer thickness that the walls most affected the shear layer instability when the convective Mach number was greater than one. As the distance between the walls decreased, the maximum amplification rate reached a maximum value and then decreased. The stability characteristics for subsonic convective Mach number waves were unaffected by wall height. Similar results were found by Morris and Giridharan [1991] and Shin and Ferziger [1993] for shear layers in a rectangular channel.

The analysis of a cylindrical supersonic vortex sheet inside a circular duct with hard walls has been performed by Viswanathan [1991], Ahuja et al. [1992], and Chang and Kuo [1993]. Viswanathan showed how the KH instabilities were affected by the wall height of a circular duct. The effect appeared as oscillations in the growth rates due to interaction between the internal Mach wave system of the jet and the reflected waves from the wall as the wall moved closer to the vortex sheet. Furthermore for a  $M_j = 4.0$  jet with no outer flow, the KH mode had growth rates typically higher than the supersonic instabilities. Chang and Kuo

found similar results for a  $M_j = 4.5$  jet with two different outer flows,  $M_o = 4.06$  and  $M_o = 1.56$ . It was also shown that the axisymmetric KH mode growth rates decreased as the outer flow velocity increased relative to the inner flow velocity. When shear layer thickness was included in the analysis (Viswanathan [1991]), the growth rates for the instabilities were diminished and the presence of the hard wall had a greater affect on KH mode growth rates than on supersonic mode growth rates.

Hu [1995] recently studied the effects of two parallel walls with sound absorbing lining on a two-dimensional jet confined inside a rectangular duct. The analysis was performed for two-dimensional instability waves with mean flow conditions  $M_j = 2.0$ ,  $M_o = 0.2$ , and  $T_j/T_o = 4.0$ . Using a vortex sheet model, the lined walls were shown to be most effective when the phase velocity was supersonic relative to the outer flow and when the pressure eigenfunction showed large perturbations near the wall. In general, growth rates were reduced when the wall impedance was finite. A continuous mean flow model based on a hyperbolic tangent function was used to include the effects of shear layer thickness. For the instability wave with the largest growth rates, the increasing shear layer thickness resulted in lower growth rates. Also, the presence of a lined wall was more effective in reducing growth rates than a hard wall.

In this paper, we extend the study of the effects of a confining wall with sound absorbing lining to the circular duct case. A  $M_j = 2.1$  axisymmetric jet mean flow is generated numerically with temperature ratio  $T_j/T_o = 2.0$ . We will only consider the Kelvin-Helmholtz type mode in this study since it is the dominant instability for both the free and confined jets at these flow conditions. The following conditions are considered in the analysis: 1) The jet has a slowly growing shear layer with axial distance. 2) The external flow in the duct is varied. 3) The wall boundary condition is varied from a solid wall to a finite impedance condition on the surface. 4) Impedances with both positive and negative imaginary parts are considered. 5) Both axisymmetric and helical modes are calculated. The study of these conditions is new to the confined jet in a circular duct that has a growing shear layer determined by a mean flow calculation with a spreading rate appropriate for the operating conditions. The next section describes the formulation of the instability wave model with a finite impedance boundary condition. The model is used to determine the growth rates and phase velocities of the instability waves that govern the pressure disturbance pattern generated by the jet shear layer. This is followed by a presentation and a discussion of the numerical results.

## 2 INSTABILITY WAVE FORMULATION

The problem of a supersonic jet inside a circular duct is illustrated in Figure 1. The high speed flow emerging from the nozzle has an initially thin shear layer that is inherently unstable even in the absence of viscosity. An instability wave begins to grow rapidly and continues to grow at reduced rates as the shear layer spreads. During this process, pressure disturbances created by the instability propagate away from the shear layer toward the wall, reflect off the wall, and return to interact with and modify the instability wave in the shear layer. This process is assumed to be governed by the linearized, inviscid, compressible equations of motion.

### 2.1 Disturbance Equations

For a slowly diverging jet flow, a locally parallel flow approximation is used to obtain the solution for the disturbance quantities. For example, the pressure disturbances are represented by

$$p'(r, \theta, x, t) = p(r, x) \times \exp \left[ i \left( \int_0^x \alpha(x) dx + n\theta - \omega t \right) \right] \quad (1)$$

where  $p(r, x)$  represents the radial distribution of the pressure disturbance at each axial location,  $\alpha(x)$  is the local complex wave number ( $\alpha = \alpha_r + i\alpha_i$  and  $-\alpha_i$  is the local growth rate),  $\theta$  is the azimuthal angle,  $n$  is the mode number, and  $\exp(-i\omega t)$  is the harmonic time dependence. The equations governing the disturbances can be combined to obtain a single second order equation,

$$\frac{\partial^2 p}{\partial r^2} + \left[ \frac{1}{r} + \frac{2\alpha}{\omega - \alpha \bar{u}} \frac{\partial \bar{u}}{\partial r} - \frac{1}{\bar{\rho}} \frac{\partial \bar{\rho}}{\partial r} \right] \frac{\partial p}{\partial r} + \left[ \bar{\rho} M_j^2 (\omega - \alpha \bar{u})^2 - \frac{n^2}{r^2} - \alpha^2 \right] p = 0 \quad (2)$$

This equation has been nondimensionalized as follows: spatial coordinates by  $R_j$ , time by  $U_j/R_j$ , velocity by  $U_j$ , density by  $\rho_j$ , and pressure by  $\rho_j U_j^2$  where the subscript  $j$  indicates jet exit conditions. The overbar quantities represent the known mean flow.

The general solution to equation (2) at any axial location is written

$$p(r) = A\zeta_1^p(r) + B\zeta_2^p(r). \quad (3)$$

Outside the jet, the mean flow becomes uniform and the solution can be written using known functions.

$$p_o = A_o H_n^{(1)}(i\lambda(\alpha)r) + B_o H_n^{(2)}(i\lambda(\alpha)r) \quad (4)$$

where

$$\lambda(\alpha) = [\alpha^2 - \bar{\rho}_o M_j^2 (\omega - \alpha \bar{u}_o)^2]^{1/2}. \quad (5)$$

$H_n^{(1)}$  is a Hankel function of the first kind. It represents a wave outgoing from the shear layer toward the wall.  $H_n^{(2)}$  is a Hankel function of the second kind and represents the wave reflected from the wall. As  $r \rightarrow 0$ , equation (3) must be finite.

At the wall, the continuity of particle displacement is used as the boundary condition (Hu [1995]). The kinematic equations are combined in terms of pressure to get

$$(\omega - \alpha \bar{u}_o)^2 p_o + \frac{i\omega}{\bar{\rho}_o} \frac{Z^*}{\rho_j U_j} \frac{\partial p_o}{\partial r} = 0 \quad (6)$$

where  $Z^*$  is the dimensional acoustic impedance. The impedance is usually referenced to a typical density and speed of sound. We use ambient conditions for density  $\rho_a$  and speed of sound  $c_a$  to get

$$\frac{Z^*}{\rho_j U_j} = Z \sqrt{\bar{\rho}_a} \frac{1}{M_j} \quad (7)$$

where  $Z = Z^*/\rho_a c_a$  is the specific acoustic impedance of the wall treatment. The wall treatment is assumed to be locally reacting. Using equation (6) at the wall, we can determine  $B_o$  in equation (4) in terms of  $A_o$ .

$$p_o = A_o \left[ H_n^{(1)}(i\lambda r) - C(h) H_n^{(2)}(i\lambda r) \right] \quad (8)$$

where

$$C(h) = \frac{(\omega - \alpha \bar{u}_o)^2 H_n^{(1)}(i\lambda h) - \frac{\omega \lambda Z \sqrt{\bar{\rho}_a}}{\bar{\rho}_o M_j} H_n^{(1)'}(i\lambda h)}{(\omega - \alpha \bar{u}_o)^2 H_n^{(2)}(i\lambda h) - \frac{\omega \lambda Z \sqrt{\bar{\rho}_a}}{\bar{\rho}_o M_j} H_n^{(2)'}(i\lambda h)}. \quad (9)$$

As  $h \rightarrow \infty$ , equation (8) reduces to the free jet case (Tam and Burton [1984]) and as  $Z \rightarrow \infty$ , the wall becomes acoustically hard and equation (8) reduces to the appropriate form obtainable from Viswanathan [1991].

Equation (2) and its boundary conditions create an eigenvalue problem with eigenvalue  $\alpha$ . The centerline

boundary condition at  $r = 0$  depends on whether the pressure eigenfunction is either axisymmetric,  $n = 0$ , or non-axisymmetric,  $n \neq 0$ . In equation form, this is written as

$$\begin{aligned}\frac{\partial p}{\partial r} &= 0, n = 0 \\ p &= 0, n \neq 0.\end{aligned}\tag{10}$$

A finite difference approximation is used to discretize equation (2) with  $A_o$  eliminated from the outer boundary condition by using a ratio of equation (8) at the two outer grid points. The local eigenvalue is found from the resulting diagonal matrix using a Newton-Raphson iteration for refinement. The local eigenfunction,  $p(r, x)$ , is then determined within a constant using the inverse power method with normalization of the eigenfunction taking place at the point where the axial mean flow velocity profile has a maximum  $\partial \bar{u} / \partial r$ . The calculations are performed at every axial location where the mean flow is determined.

## 2.2 Mean Flow

In order to complete the stability analysis, the mean flow properties are needed. Often equations consisting of simple analytic functions are used to describe the mean flow. However, in order to easily account for the effects of velocity and temperature differences across the supersonic jet shear layer on shear layer spreading, we use a numerically generated mean flow. The jet is assumed to be perfectly expanded and for the region of interest near the nozzle, the static pressure is assumed to be constant. The set of compressible, Reynolds averaged, boundary layer equations with a modified turbulence model is used as the basis for the numerical mean flow analysis. The details of the equation development, the numerical solution, and comparisons of calculated results to measured mean flow data are given in Dahl [1994].

## 3 NUMERICAL RESULTS

The calculations were performed for a jet with exit Mach number  $M_j = 2.1$ . The jet was hot relative to the outer stream with  $T_j/T_o = 2.0$ . The outer stream had the same static temperature as the ambient conditions for the source of the outer stream. The velocity ratio between the outer stream and the inner jet stream was set at three different conditions, 0.01, 0.2, and 0.4, and these operating conditions will be distinguished in the discussion of the results by referring to the outer stream Mach number  $M_o = 0.03, 0.59,$  and  $1.19$ , respectively. All the results shown in this paper are at a Strouhal number  $St = fD_j/U_j = 0.3$ , where  $D_j = 2R_j$ , since this Strouhal number was near the maximum growth rate for most of the modes of



the different operating conditions presented in this paper.

### 3.1 Solid wall

Figure 2 shows local growth rates,  $-\alpha_i$ , and phase velocities,  $c_{ph} = \omega/\alpha_r$ , for the three operating conditions at three axial locations as a function of the wall height  $h$ . The results are for the  $n = 1$  helical mode. In part (a), the jet half-width  $b$  is approximately zero and the results are similar to those obtained for a cylindrical vortex sheet in a duct (Viswanathan [1991]). The growth rate for large  $h$  is equivalent to the free jet growth rate. For  $M_o = 0.03$  and as  $h$  decreases, the growth rate has larger variations in its value. As  $M_o$  increases, this variation in growth rate gets smaller and the growth rate in general decreases. This later trend was observed in calculated results for both free jets with a coflowing stream (Michalke and Hermann [1982]) and confined cylindrical vortex sheets (Chang and Kuo [1993]). In the corresponding phase velocity plots, the branch points demarcating regions of supersonic or subsonic phase velocity relative to the flow speed are indicated for those branch points within the plotted range. Figure 3 shows the changes in the branch points as the outer flow speed changes. For a phase velocity supersonic relative to the inner stream jet velocity,

$$|1 - c_{ph}| > \frac{1}{M_j}, \quad (11)$$

and for a phase velocity supersonic relative to the outer stream,

$$|\bar{u}_o - c_{ph}| > \frac{\bar{u}_o}{M_o}. \quad (12)$$

Thus the phase velocities for the two lowest  $M_o$  cases in Figure 2(a) are supersonic relative to the outer stream. The  $M_o = 1.19$  case has subsonic relative phase velocity. All three cases have subsonic phase velocity relative to the inner stream except for the  $M_o = 0.03$  case in the region  $2.2 < h < 3$ .

As the flow moves downstream and the shear layer widens, Figures 2(b) and (c) show that the growth rates decrease but variations in the growth rate start at wall distances further from the shear layer. The phase velocities show a general increase for  $M_o < 1$ , becoming more supersonic relative to the outer stream, and a general decrease for  $M_o > 1$ , staying subsonic relative to the outer stream.

Selected eigenfunctions for pressure corresponding to the eigenvalues given in Figure 2 are shown in Figure 4 for different wall heights. For subsonic  $M_o$ , the disturbance reflection from the wall causes local minimum and maximum to appear in the eigenfunction outside the shear layer. In cases where the growth

rate decreases toward zero as  $h$  decreases, the eigenfunction takes on D family mode characteristics with supersonic phase velocity relative to the outer stream and large oscillations in the eigenfunction outside the shear layer due to reflections from the confining wall (Chang and Kuo [1993]). As  $M_o$  becomes supersonic, the eigenfunction decreases monotonically toward the wall away from the peak in the shear layer. This is evidence that the instability wave is traveling subsonically relative to the outer stream and no disturbance radiation is taking place to reflect off the confining wall. For all three cases, the eigenfunction shape inside the jet stream is little affected by reflections from the wall.

### 3.2 Lined wall

In Hu [1995], it was shown that instability wave growth rates decreased as the real part of the wall impedance decreased toward one for a fixed imaginary part and wall height. We confirmed this behavior for the circular duct case with similar operating conditions and impedance boundary conditions. For this paper, we limit our results to the case where we set  $|Z| = 1$  and vary the angle between the real and imaginary parts of  $Z$  from  $-60$  to  $+60$  degrees in the impedance plane. Thus, the real part of  $Z$  is always positive and the imaginary part is either positive or negative. These are conditions that are realizable with practical sound absorbing materials.

#### 3.2.1 Variations with Wall Height

For the case  $M_o = 0.59$  and  $b = 0.1$ , Figure 5 shows the variations of growth rates and phase velocities as the wall height changes with different wall impedances. The oscillatory variations in the growth rates appear in opposite directions as the impedance angle varies from  $-60$  to  $+60$  degrees for both  $n = 0$  and  $n = 1$  modes. Where the growth rate is minimum for  $-60$  degrees, it is near maximum for  $+60$  degrees and vice versa. A similar trend is seen in the phase velocity plots. Furthermore, the oscillations in the growth rates appear to be in a sense “90 degrees out of phase” with the oscillations in the phase velocities. When there is maximum spread in the growth rate plots with impedance angle, the phase velocities are nearly equal. Alternately, when the growth rates are nearly equal, there is maximum spread in the phase velocity plots. There are larger variations taking place for positive impedance angle than for the same negative angle.

The corresponding pressure eigenfunctions for selected wall heights are shown in Figure 6 for the different impedance conditions and for both  $n = 0$  and  $n = 1$  modes. As can be seen, for positive impedance angles, the eigenfunction approaches the wall with increasing amplitude and for negative impedance angles, the

eigenfunction approaches the wall with decreasing amplitude. This was observed at all wall heights selected for study. The effect of the impedance boundary condition to reduce reflections is evident in the decrease of the onset of D family modes seen in the solid wall results for  $h = 2$  in both  $n = 0$  and  $n = 1$  plots. The eigenfunctions tend to hold their KH characteristic, except for the  $-60$  degree impedance condition at  $h = 2$ ,  $n = 0$  where the peak of the eigenfunction is outside the shear layer. We can see that the majority of the variations in the eigenfunction with wall impedance angle take place outside the shear layer and little variation takes place inside the jet.

### 3.2.2 Variations with Axial Distance

Figure 7 shows variations in growth rate and phase velocity with axial distance for a fixed wall height of  $h = 2$ . In the horizontal direction, the KH mode number  $n$  varies from 0 to 2 and in the vertical direction, the three outer stream Mach number cases are given. The axial distance is labeled in terms of the jet half-width  $b$  of the shear layer. The horizontal lines in the phase velocity plots indicate the locations of the branch points as described in Figure 3. For the low speed outer stream case  $M_o = 0.03$ , the growth rates decrease as the wall impedance decreases as noted by Hu [1995]. However, as  $M_o$  increases, the growth rates for the cases with finite wall impedance can become higher than the solid wall growth rates. Less change in the growth rates occur as the outer flow increases and as the mode number increases.

The phase velocities are mostly supersonic relative to the outer stream and subsonic relative to the inner stream. The phase velocity decreases as mode number and outer stream Mach number increase. For  $M_o = 0.03$ , the phase velocity becomes supersonic relative to the inner stream as the phase velocity decreases. For  $M_o = 1.19$ , the phase velocity becomes subsonic relative to the outer stream. As seen in the growth rate plots, the lined wall has a decreasing effect on phase velocity as mode number or  $M_o$  increase.

The combination of the eigenvalue and the eigenfunction create the pressure disturbance pattern generated by the jet shear layer instability wave in the duct. Using the real part of equation (1) with the amplitude normalized to 1 for the peak of the initial eigenfunction nearest the nozzle exit, the spatial pressure disturbance patterns for the free jet case and for the solid wall and the lined wall cases with  $Z = 1$  are shown as equal pressure contours in Figure 8 where  $h = 2$ . The mode number  $n$  is 1 and the outer stream Mach number is 0.59. The free jet disturbances radiate acoustic energy to the far field since the phase velocities are supersonic relative to the ambient speed of sound. Thus, the energy escapes the system and does not return

to affect the instability wave characteristics. When a solid wall is placed at  $h = 2$ , the effect of reflections from the wall are easily seen in the contour plots as increased pressure levels near the wall. When the wall has the impedance condition  $Z = 1$ , the reflections are reduced and the pressure disturbance pattern is similar to the free jet pattern except near the wall and downstream where the amplitudes are slightly higher due to slightly larger growth rates. In general, the free jet and the lined wall cases have similar growth rates and phase velocities. When the wall is hard, the growth rates decreased from the  $Z = 1$  growth rates and the phase velocities increased (see center plot of Figure 7). This increase in phase velocity results in the noticeable increase in wavelength shown in Figure 8 for the solid wall case compared to either the free jet or lined wall cases.

Finally, pressure disturbance patterns are shown in Figure 9 for changes in the wall impedance angle. When the angle is positive, the pressure eigenfunction approaches the wall with increasing amplitude (Figure 6). At  $+60$  degrees, this leads to greater reflections from the wall as the flow proceeds downstream, compared to the  $Z = 1$  case, and greater amplitudes due to greater growth rates in the axial direction. When the angle is  $-60$  degrees, the growth rates are lessened and reflections do not appear in the disturbance pattern over the axial distance shown in the figure.

#### 4 DISCUSSION

For a solid wall confining duct, our analysis confirms that the growth rates of Kelvin-Helmholtz type instability waves are affected by wall height when the waves have phase velocities supersonic relative to the outer flow. There is little affect when the phase velocities are subsonic relative to the outer flow. Our results agree with Chang and Kuo [1993] for the cylindrical vortex sheet case in a solid wall duct where the growth rates generally decrease with an increase in the outer flow. As the shear layer widens, growth rates decrease. But, as the wall height changes, growth rates can increase or decrease with an outer flow increase. Thus, there is no direct correlation found between growth rates and outer flow velocity for wider shear layers as there is for the vortex sheet case.

Hu [1995] found that growth rates for two-dimensional instability waves decreased when the real part of the rectangular duct wall impedance was decreased from infinity (solid wall) to one. This occurred at a relatively low speed,  $M_o = 0.2$ , outer flow. Our results show in Figure 7 that this trend is not followed for circular ducts with higher outer flow velocities and with higher order mode instability waves. As the

outer flow increases, the phase velocities become less supersonic relative to the outer flow and the growth rates for the impedance wall boundary condition can be higher than the solid wall growth rates. Higher modes decay more rapidly away from the shear layer than lower order modes, thus, they are less affected by the wall boundary condition. Upon closer examination of the results given in Hu [1995], we find that the two-dimensional, rectangular duct data appear to be consistent with the axisymmetric  $n = 0$  mode, lower  $M_o$  results in Figure 7; however, further calculations are required for confirmation. Thus, our results are an extension of the previous results on the effects of an impedance wall boundary condition to the conditions of both higher, non-axisymmetric modes and higher outer mean flows.

Impedance boundary conditions at the wall reduce reflections and in some cases simulate the free jet environment in terms of growth rates, phase velocities, and pressure disturbance patterns. Setting the wall impedance  $|Z| = 1.0$  and changing the angle of the impedance to produce positive and negative imaginary parts affects the stability characteristics of the instability wave and the pressure disturbance pattern. For the wall nearer to the shear layer, growth rates are reduced for negative imaginary parts and enhanced for positive imaginary parts. This also affects reflections from the wall. For positive imaginary part, the pressure disturbance increases in amplitude near the wall creating larger reflections than when the wall impedance has a negative imaginary part. For the latter, the pressure disturbance decreases in amplitude near the wall. Thus for negative imaginary part, growth rates are reduced and the overall growth of the instability wave is reduced leading to less pressure disturbance levels. This can result in less noise radiated out from a finite length duct.

## REFERENCES

- K. K. Ahuja, K. C. Massey, A. J. Fleming, C. K. W. Tam, and R. R. Jones III. Acoustic Interactions Between an Altitude Test Facility and Jet Engine Plumes – Theory and Experiments. TR-91-20, AEDC, 1992.
- C. C. Chang and C. Y. Kuo. Instability of a Supersonic Vortex Sheet Inside a Circular Duct. *Phys. Fluids A*, 5:2217–2228, 1993.
- M. D. Dahl. *The Aeroacoustics of Supersonic Coaxial Jets*. PhD thesis, Penn State University, 1994.
- F. Q. Hu. The Acoustic and Instability Waves of Jets Confined Inside an Acoustically Lined Rectangular Duct. *J. Sound Vib.*, 183:841–856, 1995.
- A. Michalke and G. Hermann. On the Inviscid Instability of a Circular Jet with External Flow. *J. Fluid Mech.*, 114:343–359, 1982.

- P. J. Morris and M. G. Giridharan. The Effect of Walls on Instability Waves in Supersonic Shear Layers. *Phys. Fluids A*, 3:356–358, 1991.
- D. S. Shin and J. H. Ferziger. Linear Stability of the Confined Compressible Reacting Mixing Layer. *AIAA J.*, 31:571–577, 1993.
- C. K. W. Tam and D. E. Burton. Sound Generated by Instability Waves of Supersonic Flows. Part 2. Axisymmetric Jets. *J. Fluid Mech.*, 138:273–295, 1984.
- C. K. W. Tam and F. Q. Hu. The Instability and Acoustic Wave Modes of Supersonic Mixing Layers Inside a Rectangular Channel. *J. Fluid Mech.*, 203:51–76, 1989.
- K. Viswanathan. *Turbulent Mixing in Supersonic Jets*. PhD thesis, Penn State University, 1991.
- M. Zhuang, P. E. Dimotakis, and T. Kubota. The Effect of Walls on a Spatially Growing Supersonic Shear Layer. *Phys. Fluids A*, 2:599–604, 1990.

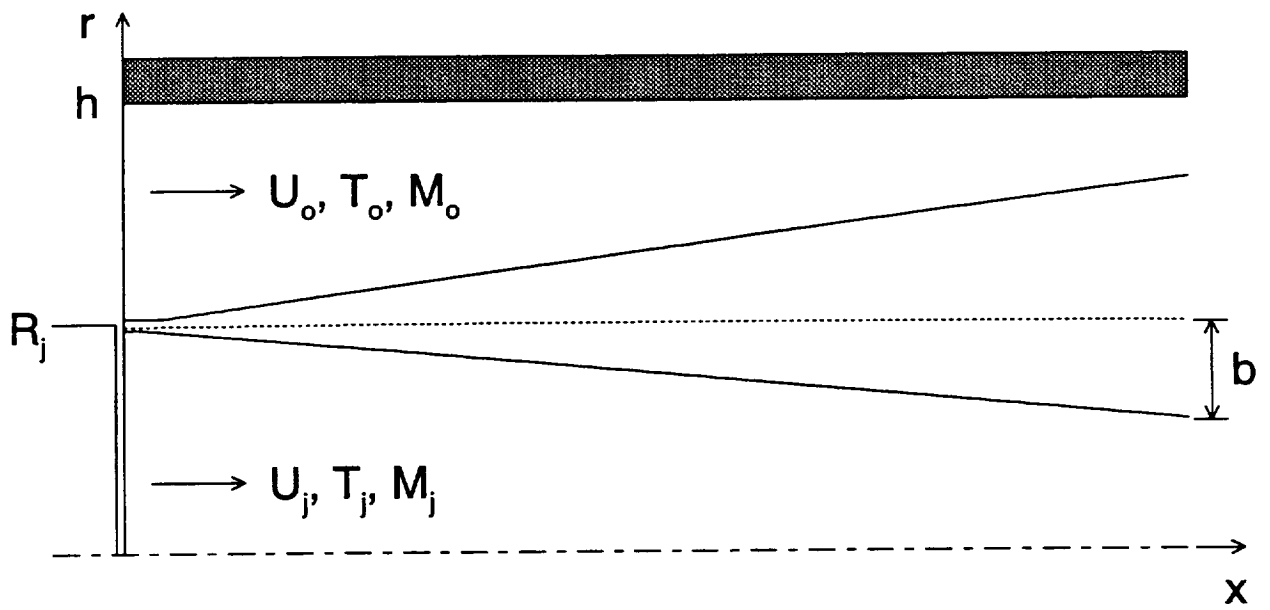


Figure 1: Schematic diagram in the  $x$ - $r$  plane of an axisymmetric jet flowing into a circular duct with coflowing outer stream.

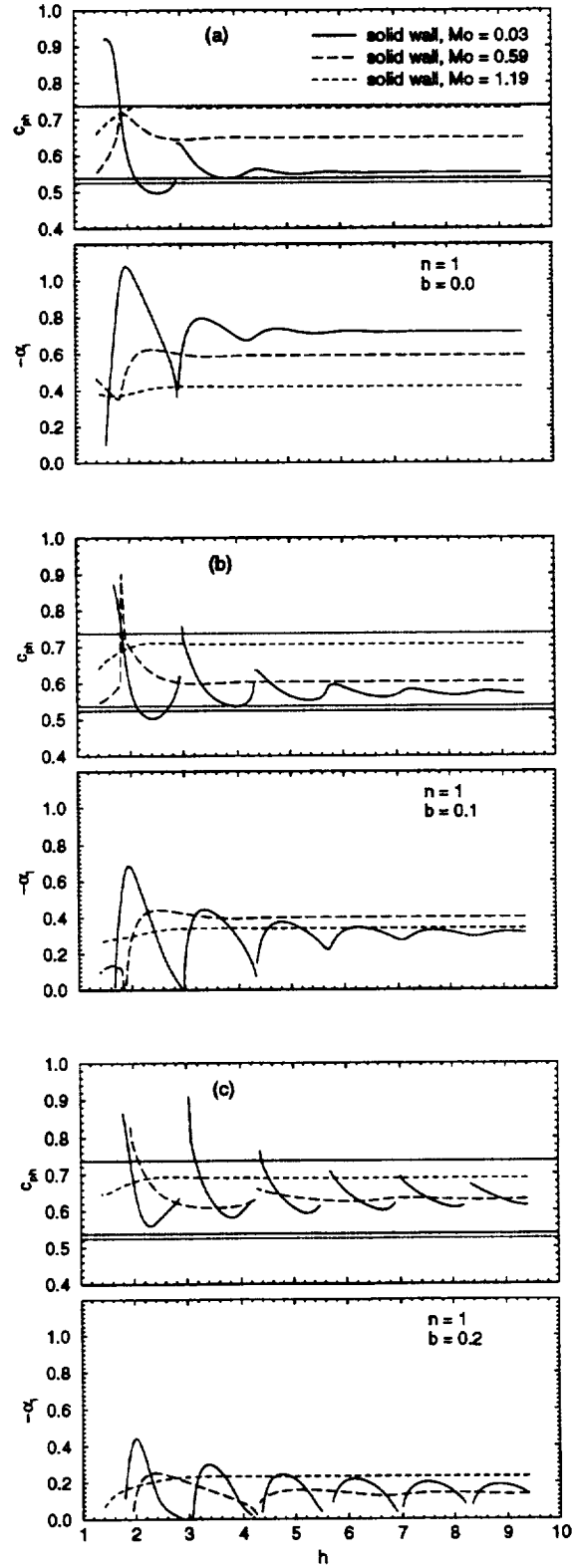


Figure 2: Local growth rates and phase velocities for the  $n = 1$  mode of an  $M_j = 2.1$  axisymmetric jet in a solid wall circular duct. Each plot shows results for three different outer flow speeds as a function of wall height. Axial locations are where (a)  $b \approx 0.0$ , (b)  $b = 0.1$ , and (c)  $b = 0.2$ .



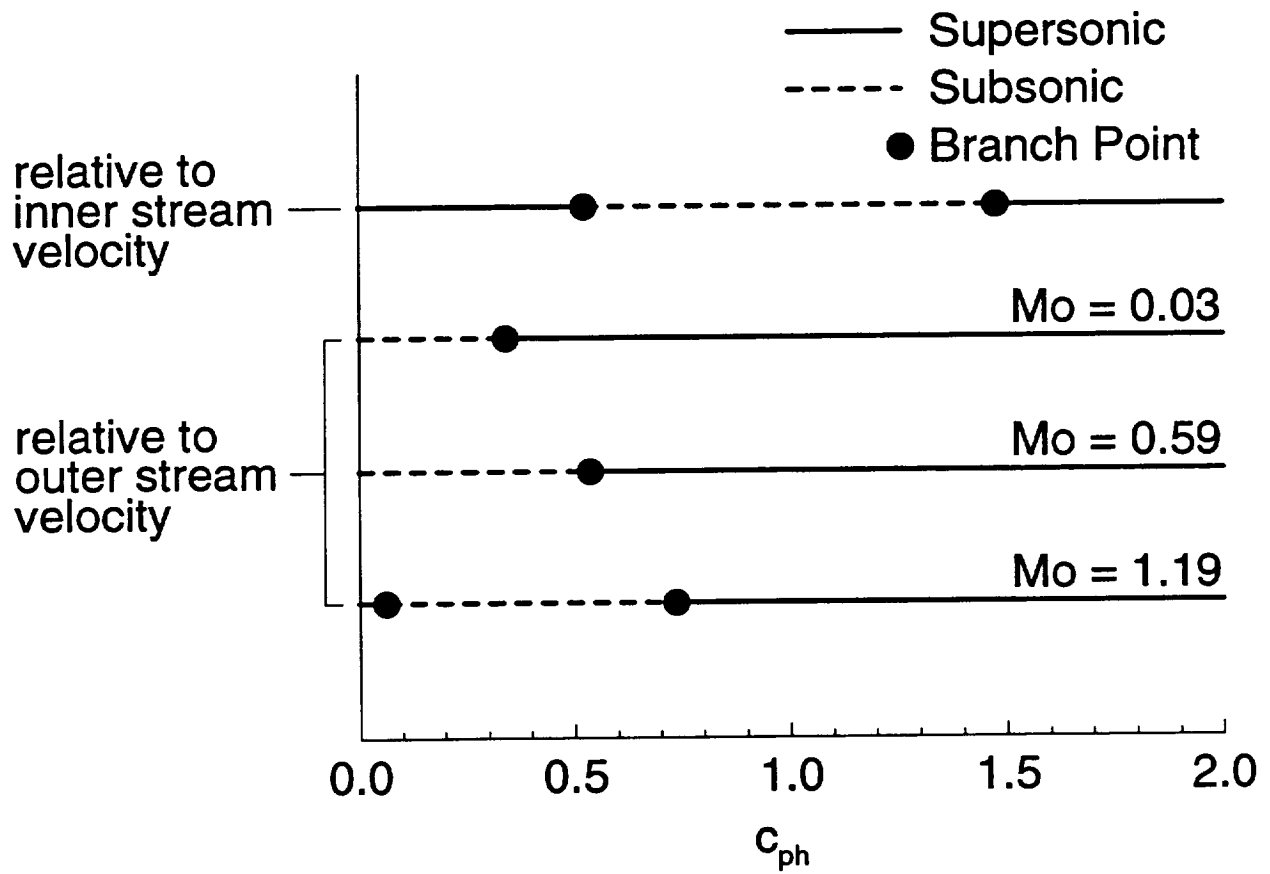


Figure 3: Branch points between regions of supersonic and subsonic phase velocity relative to the flow speed.

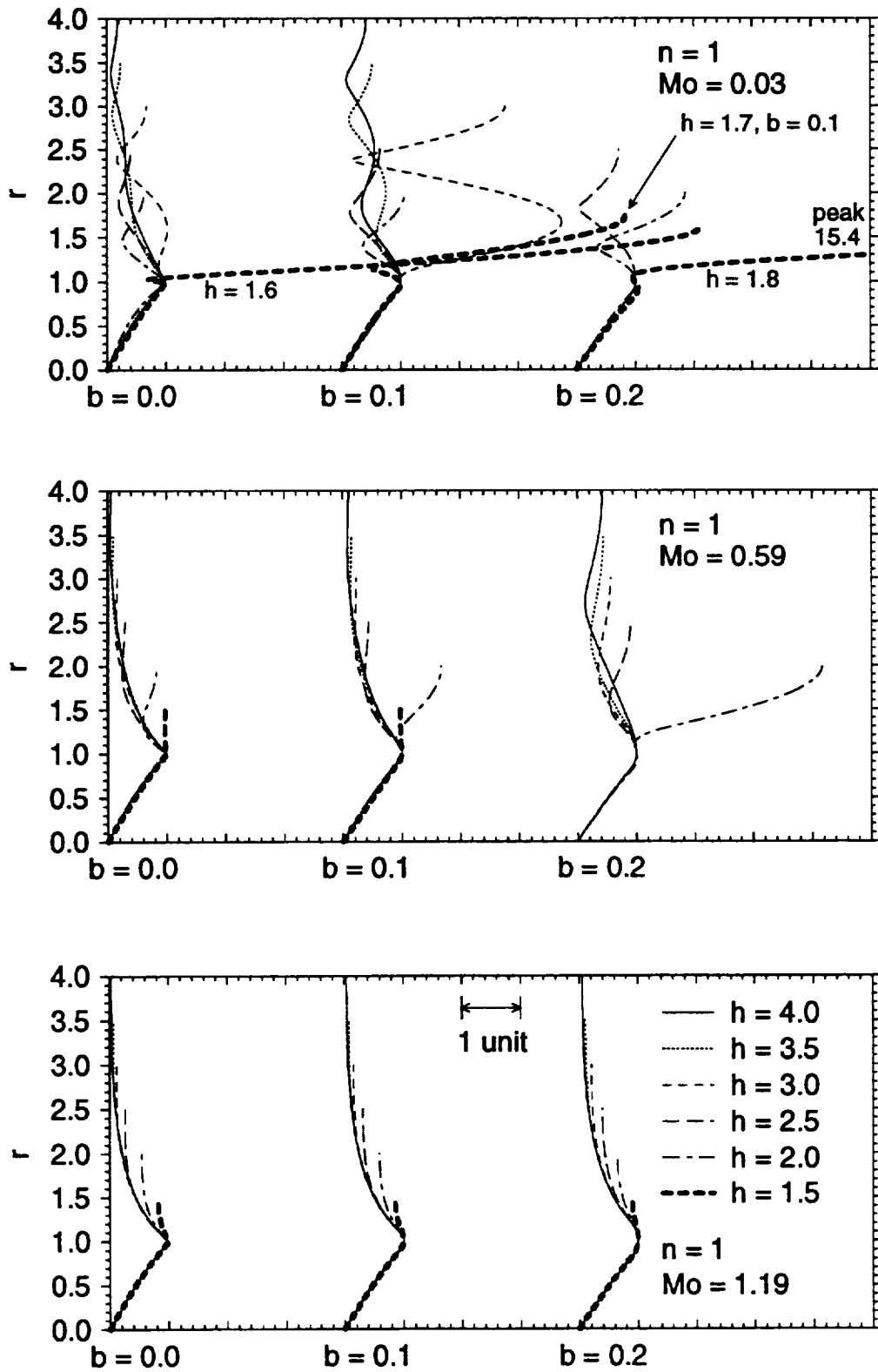


Figure 4: Pressure eigenfunctions at selected wall heights for the eigenvalues shown in Figure 2.

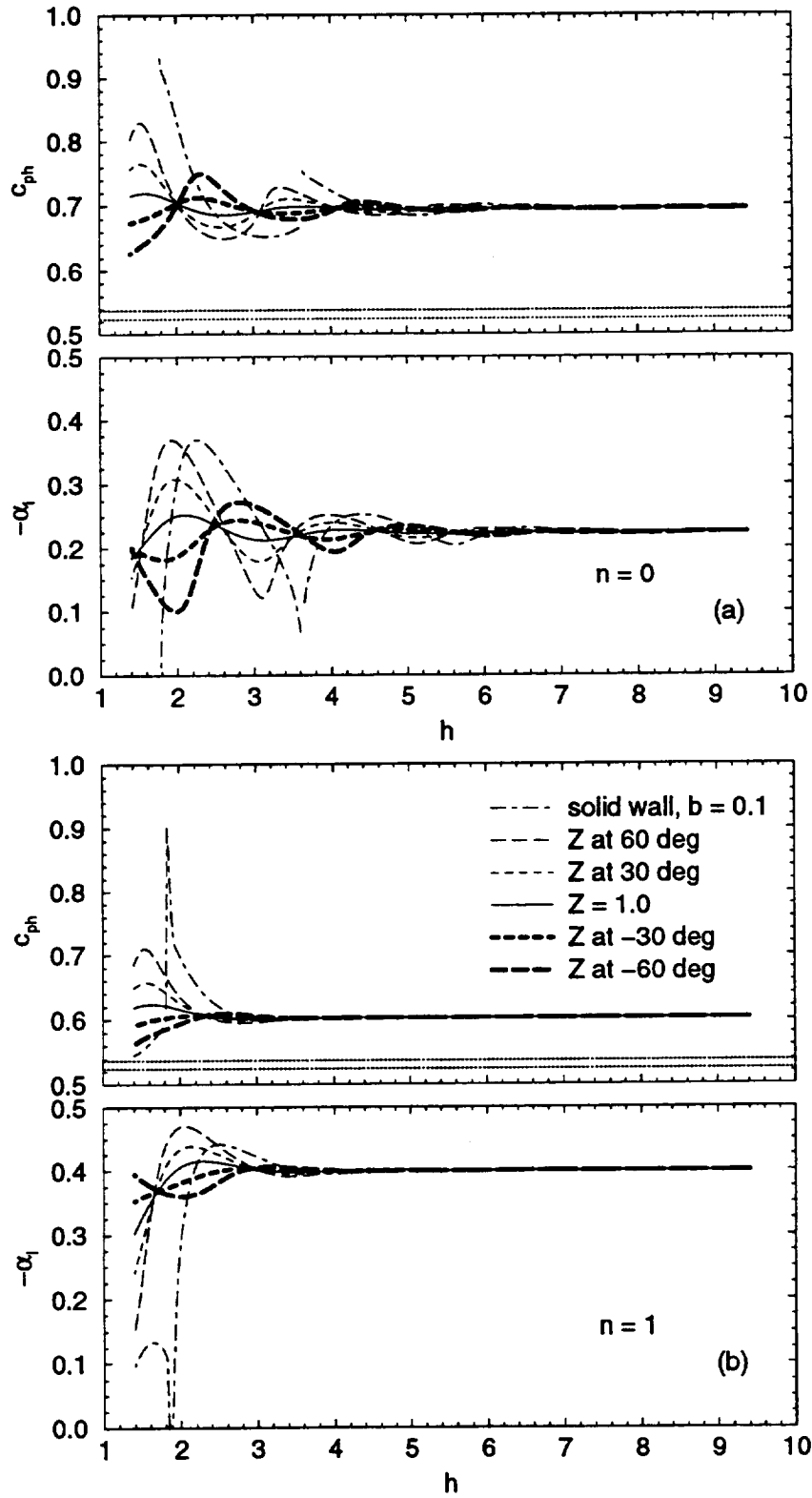


Figure 5: Local growth rates and phase velocities for an axisymmetric jet in a circular duct at  $b = 0.1$  as a function of wall height.  $M_j = 2.1$ ,  $M_o = 0.59$ ,  $|Z| = 1.0$ , impedance angle varies. (a)  $n = 0$ , (b)  $n = 1$

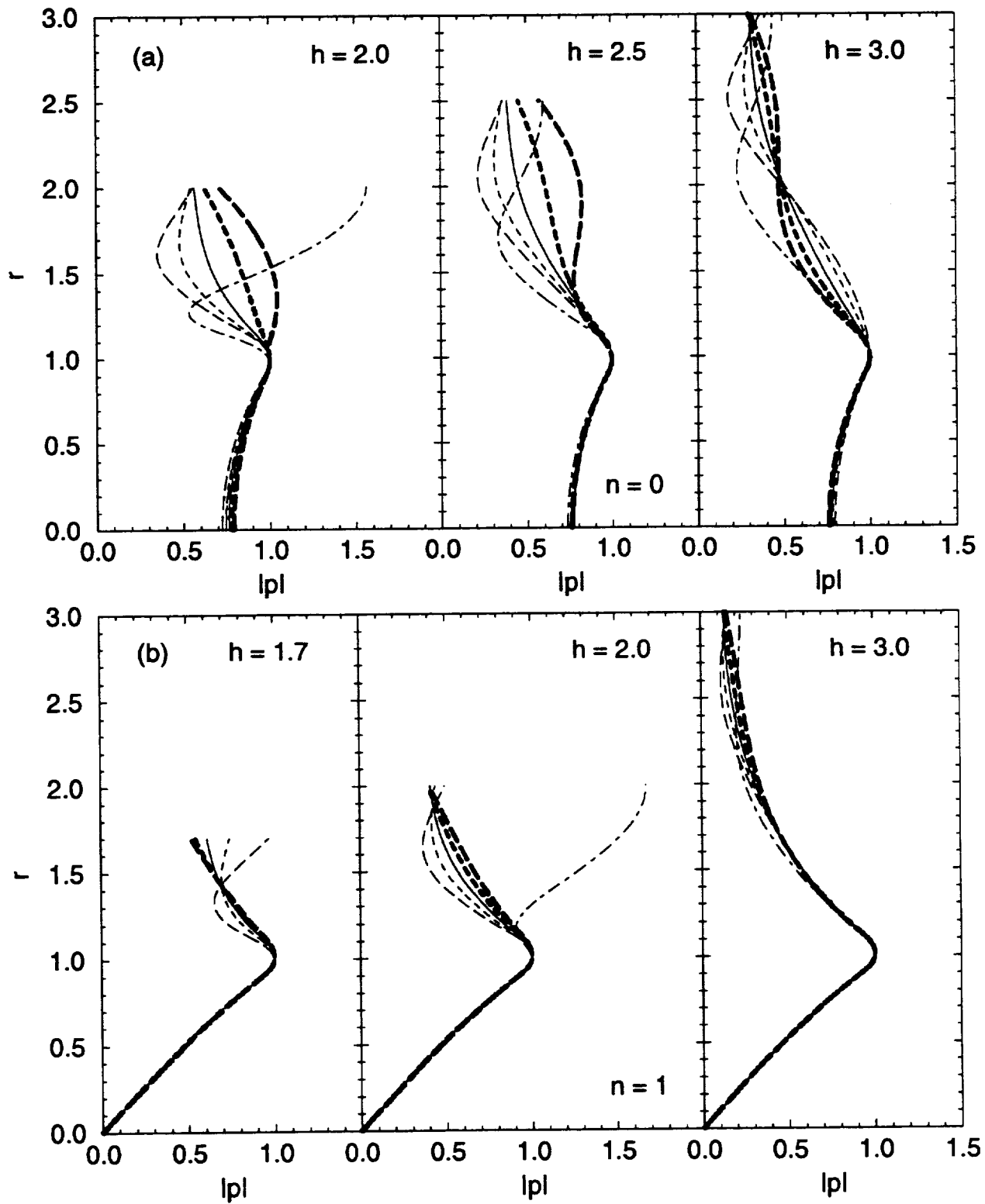


Figure 6: Pressure eigenfunctions at selected wall heights for the eigenvalues shown in Figure 5 with legend. (a)  $n = 0$ , (b)  $n = 1$

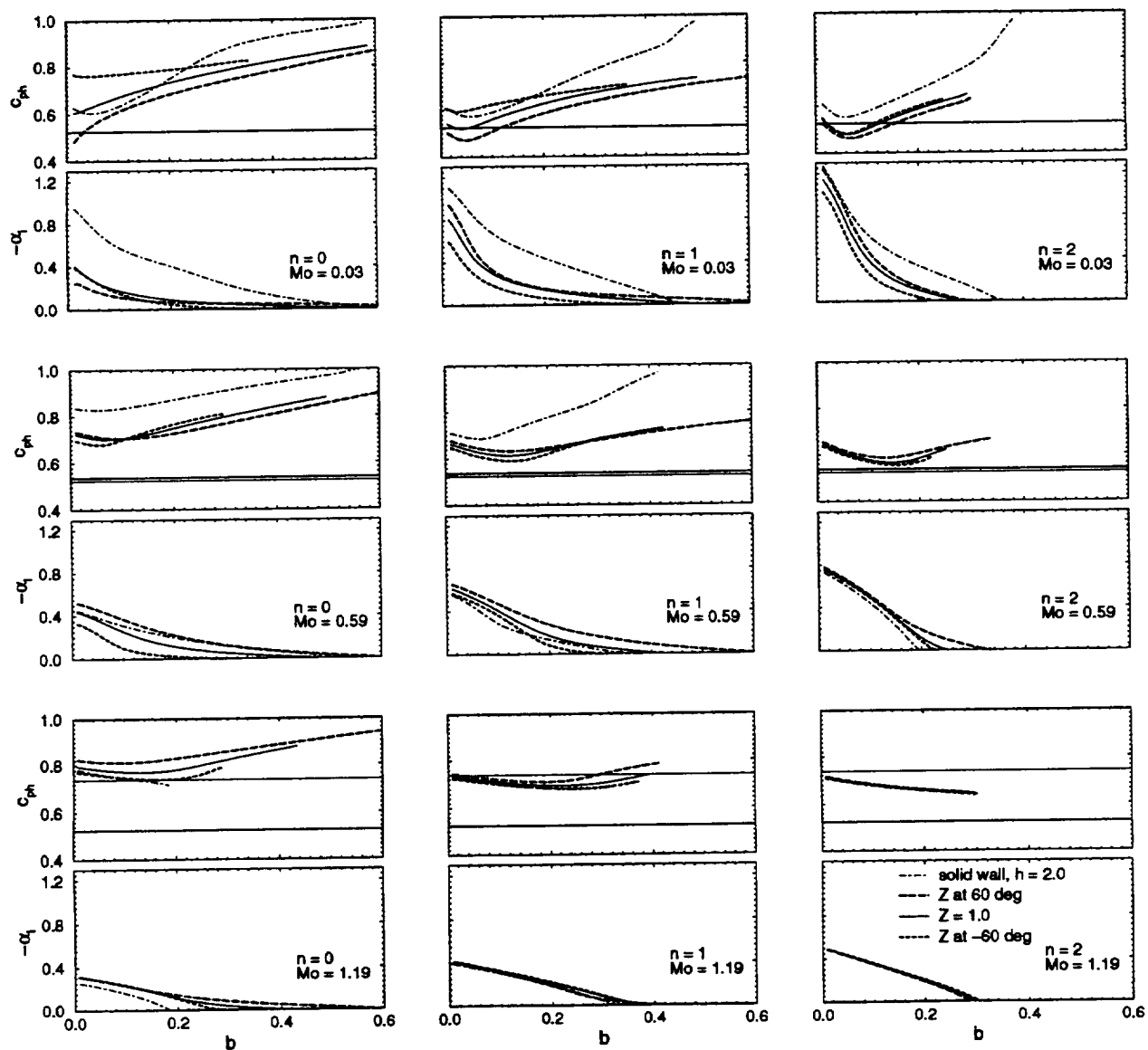


Figure 7: Growth rates and phase velocities as a function of jet half-width for a  $M_j = 2.1$  jet in a circular duct with  $h = 2.0$ .  $|Z| = 1.0$ . Impedance angle varies. KH mode number varies in horizontal direction. Outer flow speed varies in vertical direction.

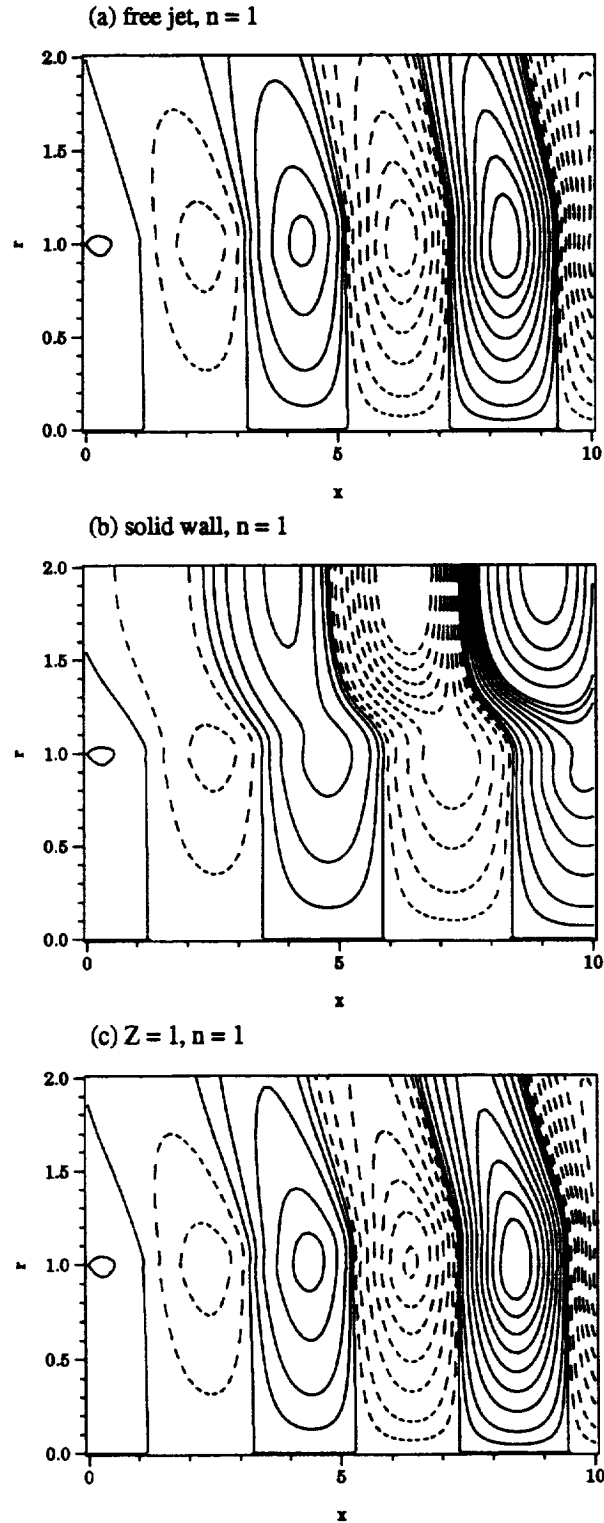


Figure 8: Spatial pressure disturbance patterns shown with equal pressure contours. Contours at  $0, \pm 1$ , steps of 2.5 for  $|p| \leq 20$ , steps of 10 for  $|p| > 20$ . Solid line,  $|p| \geq 0$ . Dashed line,  $|p| < 0$ . KH mode  $n = 1$  has zero amplitude along centerline.  $M_j = 2.1, M_o = 0.59$ . (a) free jet, (b) solid wall,  $h = 2.0$ , (c) lined wall,  $h = 2.0, Z = 1.0$

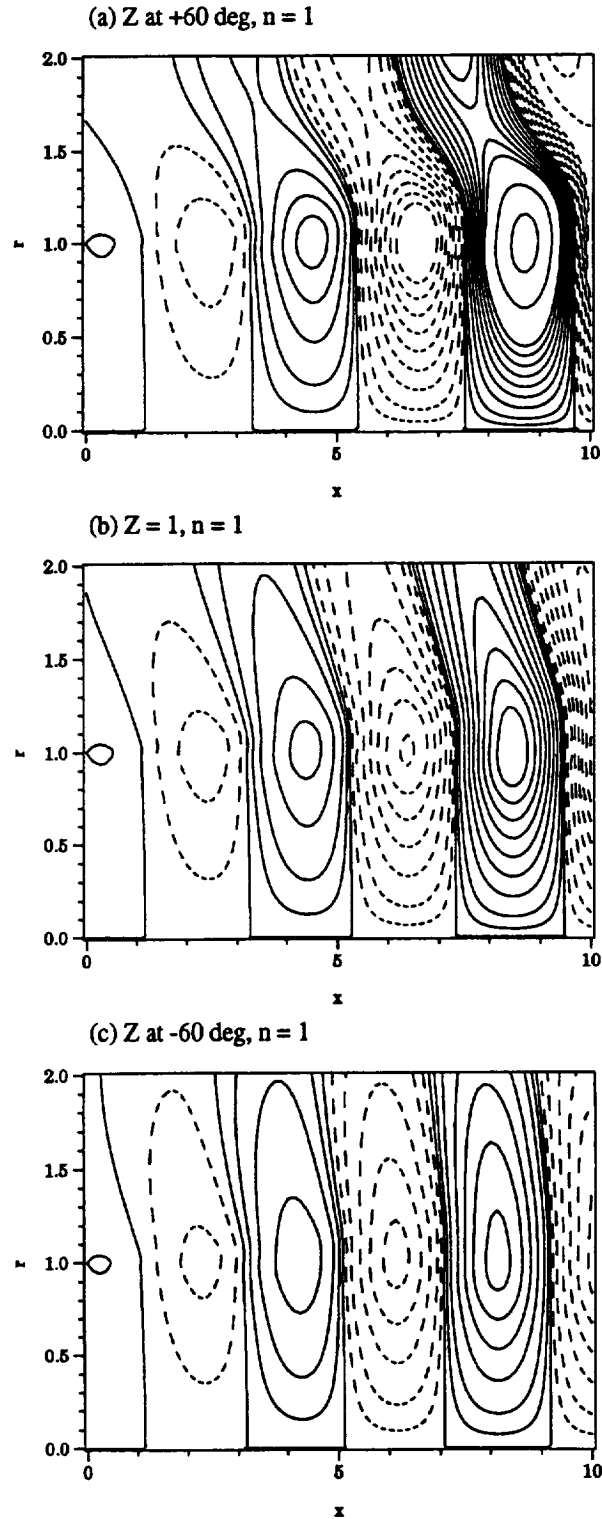


Figure 9: Spatial pressure disturbance patterns shown with equal pressure contours. Contours at  $0, \pm 1$ , steps of 2.5 for  $|p| \leq 20$ , steps of 10 for  $|p| > 20$ . Solid line,  $|p| \geq 0$ . Dashed line,  $|p| < 0$ . KH mode  $n = 1$  has zero amplitude along centerline.  $M_j = 2.1$ ,  $M_o = 0.59$ . Lined wall  $h = 2.0$ , (a)  $Z = 0.5 + i0.866$ , (b)  $Z = 1.0$ , (c)  $Z = 0.5 - i0.866$

# REPORT DOCUMENTATION PAGE

Form Approved  
OMB No. 0704-0188

Public reporting burden for this collection of information is estimated to average 1 hour per response, including the time for reviewing instructions, searching existing data sources, gathering and maintaining the data needed, and completing and reviewing the collection of information. Send comments regarding this burden estimate or any other aspect of this collection of information, including suggestions for reducing this burden, to Washington Headquarters Services, Directorate for Information Operations and Reports, 1215 Jefferson Davis Highway, Suite 1204, Arlington, VA 22202-4302, and to the Office of Management and Budget, Paperwork Reduction Project (0704-0188), Washington, DC 20503.

<b>1. AGENCY USE ONLY (Leave blank)</b>		<b>2. REPORT DATE</b> November 1996	<b>3. REPORT TYPE AND DATES COVERED</b> Technical Memorandum	
<b>4. TITLE AND SUBTITLE</b> The Effects of Acoustic Treatment on Pressure Disturbances From a Supersonic Jet in a Circular Duct			<b>5. FUNDING NUMBERS</b>  WU-505-62-52	
<b>6. AUTHOR(S)</b> Milo D. Dahl			<b>8. PERFORMING ORGANIZATION REPORT NUMBER</b>  E-10513	
<b>7. PERFORMING ORGANIZATION NAME(S) AND ADDRESS(ES)</b>  National Aeronautics and Space Administration Lewis Research Center Cleveland, Ohio 44135-3191				
<b>9. SPONSORING/MONITORING AGENCY NAME(S) AND ADDRESS(ES)</b>  National Aeronautics and Space Administration Washington, DC 20546-0001			<b>10. SPONSORING/MONITORING AGENCY REPORT NUMBER</b>  NASA TM-107358	
<b>11. SUPPLEMENTARY NOTES</b> Prepared for the International Mechanical Engineering Congress and Exposition sponsored by the American Society of Mechanical Engineers, Atlanta, Georgia, November 17-22, 1996. Responsible person, Milo D. Dahl, organization code, 2660, (216) 433-3578.				
<b>12a. DISTRIBUTION/AVAILABILITY STATEMENT</b>  Unclassified - Unlimited Subject Category 34  This publication is available from the NASA Center for AeroSpace Information, (301) 621-0390.			<b>12b. DISTRIBUTION CODE</b>	
<b>13. ABSTRACT (Maximum 200 words)</b>  The pressure disturbances generated by an instability wave in the shear layer of a supersonic jet are studied for an axisymmetric jet inside a lined circular duct. For the supersonic jet, locally linear stability analysis with duct wall boundary conditions is used to calculate the eigenvalues and the eigenfunctions at each axial location. These values are used to determine the growth rates and phase velocities of the instability waves and the near field pressure disturbance patterns. The study is confined to the dominant Kelvin-Helmholtz instability mode and to the region just downstream of the nozzle exit where the shear layer is growing but is still small in size compared to the radius of the duct. Numerical results are used to study the effects of changes in the outer flow, growth in the shear layer thickness, wall distance, and wall impedance, and the effects of these changes on non-axisymmetric modes. The primary results indicate that the effects of the duct wall on stability characteristics diminish as the outer flow increases and as the jet azimuthal mode number increases. Also, wall reflections are reduced when using a finite impedance boundary condition at the wall; but in addition, reflections are reduced and growth rates diminished by keeping the imaginary part of the impedance negative when using the negative exponential for the harmonic dependence.				
<b>14. SUBJECT TERMS</b> Supersonic jets; Acoustic treatment; Ejectors; Confined jets; Instability waves			<b>15. NUMBER OF PAGES</b> 23	
			<b>16. PRICE CODE</b> A03	
<b>17. SECURITY CLASSIFICATION OF REPORT</b> Unclassified	<b>18. SECURITY CLASSIFICATION OF THIS PAGE</b> Unclassified	<b>19. SECURITY CLASSIFICATION OF ABSTRACT</b> Unclassified	<b>20. LIMITATION OF ABSTRACT</b>	